iScience

CellPress

Article

Repression of G1/S Transition by Transient Inhibition of miR-10404 Expression in *Drosophila* Primordial Germ Cells

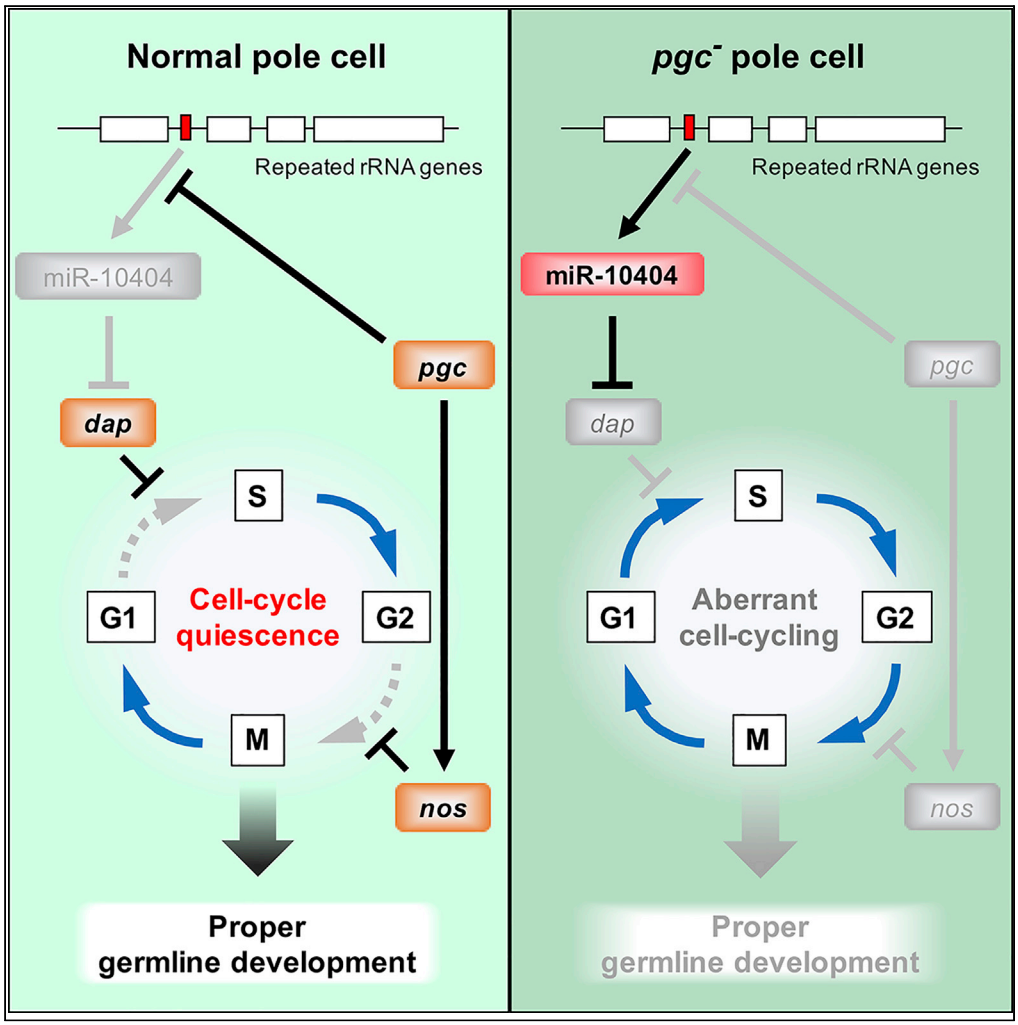

Shumpei Morita, Ryoma Ota, Makoto Hayashi, Satoru Kobayashi

skob@tara.tsukuba.ac.jp

HIGHLIGHTS

Expression of *mir-10404* encoded by rDNA region was increased in *pgc*⁻ pole cells

Increased miR-10404 expression caused premature degradation of maternal *dap* mRNA

Premature degradation of maternal *dap* mRNA derepressed G1/S transition in pole cells

Derepression of G1/S transition impaired proper germline development

Morita et al., iScience *23*, 100950
March 27, 2020 © 2020 The Author(s).
https://doi.org/10.1016/j.isci.2020.100950

iScience

CellPress

Article

Repression of G1/S Transition by Transient Inhibition of miR-10404 Expression in *Drosophila* Primordial Germ Cells

Shumpei Morita,[1,2,3] Ryoma Ota,[2] Makoto Hayashi,[1,2] and Satoru Kobayashi[1,2,4,*]

SUMMARY

Cell-cycle quiescence is a common feature of early germline development in many animal species. In *Drosophila* germline progenitors (pole cells), both G2/M and G1/S transitions are blocked. G2/M transition is repressed by maternal Nanos through suppression of Cyclin B production. However, the molecular mechanism underlying blockage of G1/S transition remains elusive. We found that repression of miR-10404 expression is required to block G1/S transition in pole cells. Expression of miR-10404, a microRNA encoded within the internal transcribed spacer 1 of rDNA, is repressed in early pole cells by maternal *polar granule component*. This repression delays the degradation of maternal *dacapo* mRNA, which encodes an inhibitor of G1/S transition. Moreover, derepression of G1/S transition in pole cells causes defects in their maintenance and their migration into the gonads. Our observations reveal the mechanism inhibiting G1/S transition in pole cells and its requirement for proper germline development.

INTRODUCTION

In *Drosophila*, maternal factors required for germline development are localized in pole plasm at the posterior pole of the cleavage embryos and are partitioned into the primordial germ cells, called as pole cells (Illmensee and Mahowald, 1974). The pole cells remain at the posterior pole region of the blastoderm embryos and then migrate through embryos to reach the somatic gonads, where they differentiate into functional gamete (Richardson and Lehmann, 2010). Once pole cells initiate migration, cell cycling is arrested at the G2 phase until they reach the somatic gonads, whereas somatic cells continue to proliferate during embryogenesis (Asaoka-Taguchi et al., 1999; Sonnenblick, 1941; Su et al., 1998; Technau and Campos-Ortega, 1986; Underwood et al., 1980). Although cell-cycle quiescence of germline cells has been reported in many animal species, including *Drosophila* (Asaoka-Taguchi et al., 1999; Fukuyama et al., 2006; Juliano et al., 2010; Kalt and Joseph, 1974; Seki et al., 2007; Su et al., 1998), its regulatory mechanism is poorly understood.

It has been reported that Nanos (Nos) protein produced from maternal *nos* mRNA inhibits G2/M transition in pole cells by suppressing translation of maternal *Cyclin B* (*CycB*) mRNA (Asaoka-Taguchi et al., 1999; Kadyrova et al., 2007). Lack of maternal Nos activity or CycB protein overexpression is able to drive the quiescent pole cells through mitosis (Asaoka-Taguchi et al., 1999). However, the prematurely induced mitosis in pole cells is never followed by the S phase, and the pole cells are arrested again at the G1 phase (Asaoka-Taguchi et al., 1999; Su et al., 1998). This indicates that G1/S transition is also arrested in pole cells and this arrest is independent of Nos activity. Thus, continued cell cycling of pole cells is tightly blocked through multiple cell-cycle checkpoints, or G2/M and G1/S transition. This leads us to speculate that cell-cycle quiescence plays a critical role in germline development.

In this study, we report a mechanism by which G1/S transition is blocked in the migrating pole cells. Our key findings are as follows: (1) In early pole cells, maternal *polar granule component* (*pgc*) represses nucleolus formation and expression of miR-10404 encoded within Nucleolus Organizer Region (NOR). (2) *pgc*-mediated repression of miR-10404 delays degradation of *dacapo* (*dap*) mRNA, which in turn blocks G1/S transition in the migrating pole cells. (3) Derepression of both G1/S and G2/M transition induced by miR-10404 and *CycB* in pole cells causes their failure to migrate properly into the gonads, and their elimination in embryos, implying the importance of the cell-cycle quiescence in *Drosophila* germline development. Considering that cell-cycle quiescence is a common feature of germline development among animals (Nakamura and Seydoux, 2008), our findings provide a basis for understanding the mechanism and significance of cell-cycle quiescence in germline development.

[1]Graduate School of Life and Environmental Sciences, University of Tsukuba, Tsukuba, Ibaraki 305-8572, Japan

[2]Life Science Center for Survival Dynamics, Tsukuba Advanced Research Alliance (TARA), University of Tsukuba, Tsukuba, Ibaraki 305-8577, Japan

[3]Present address: Molecular Biology, Cell Biology and Biochemistry (MCB), Brown University, Providence, RI 02906, USA

[4]Lead Contact

*Correspondence: skob@tara.tsukuba.ac.jp

https://doi.org/10.1016/j.isci.2020.100950

This is an open access article under the CC BY-NC-ND license (http://creativecommons.org/licenses/by-nc-nd/4.0/).

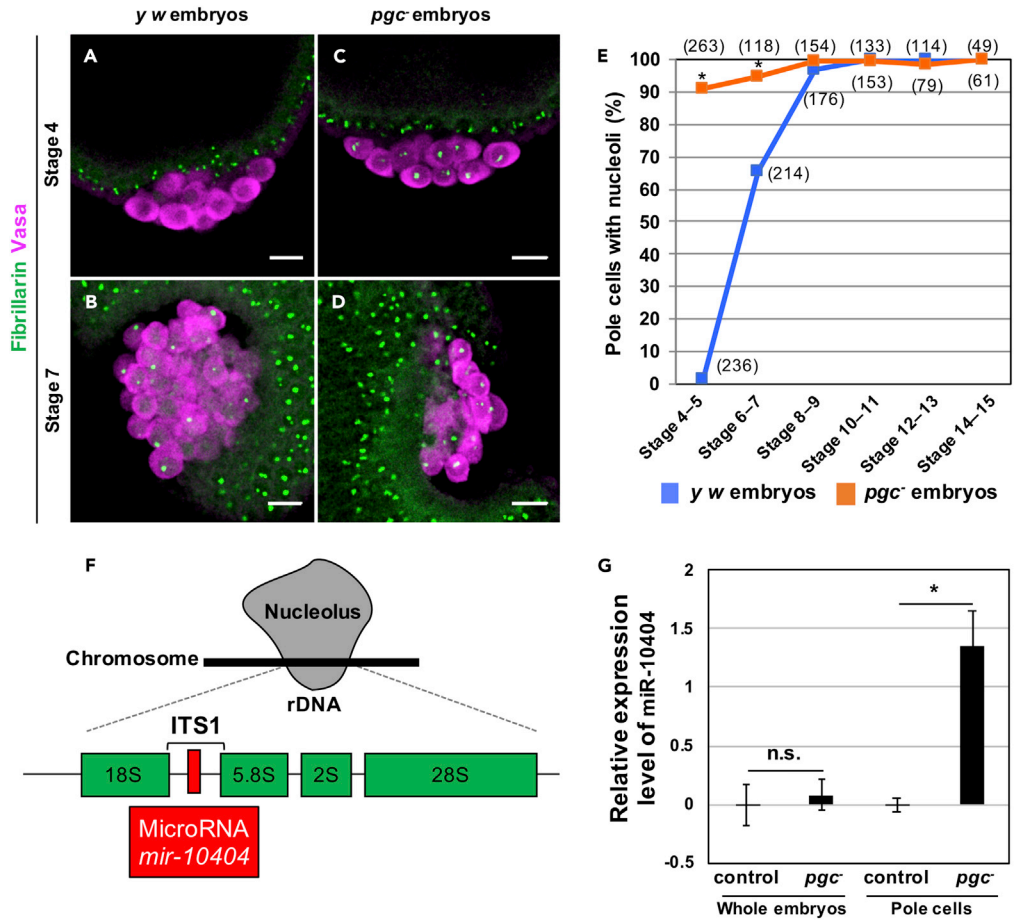

Figure 1. Derepression of Nucleolar Formation and miR-10404 Expression in *pgc*⁻ Pole Cells

(A–D) *y w* (A and B) and *pgc*⁻ (C and D) embryos at stage 4 (A and C) and 7 (B and D) were immunostained for fibrillarin, a marker for nucleoli (green), and Vasa, a marker for pole cells (magenta). Scale bars: 10 μm.

(E) Percentage of pole cells with nucleoli in *y w* (blue) and *pgc*⁻ (orange) embryos, plotted against embryonic stage. The numbers of *y w* and *pgc*⁻ pole cells examined at each stage are shown in parentheses. Significance was calculated between *y w* and *pgc*⁻ by Fisher's exact test (*: $p < 0.01$).

(F) Schematic diagram of *mir-10404* gene. *mir-10404* is encoded within the ITS1 region encompassed by the 18S and 5.8S rRNA genes. Nucleolus (gray), *mir-10404* gene (red), and rRNA genes (green) are shown.

(G) Relative expression level of miR-10404 in pole cells and whole embryos derived from *pgc/+* (control) and *pgc/pgc* (*pgc*⁻) females. RT-qPCR was performed to detect miR-10404 and *rp49* mRNA in control and *pgc*⁻ whole embryos and in 200 pole cells from control and *pgc*⁻ embryos. The amount of miR-10404 in each sample was normalized against the corresponding amount of *rp49* mRNA and is represented as a $\log_2$(fold change) relative to the level of miR-10404 in controls. Error bars indicate standard errors of three biological replicates. Significance was calculated between control and *pgc*⁻ by Student's t test (n.s.: $p > 0.05$, *: $p < 0.05$).

RESULTS AND DISCUSSION

miR-10404 Expression Is Inhibited by Maternal *pgc* in Early Pole Cells

A previous electron microscopic study revealed that newly formed pole cells lack nucleoli at the blastoderm stage, whereas the rest of the somatic nuclei have prominent nucleoli (Mahowald, 1968). To determine the embryonic stage at which pole cells initiate nucleolar formation, we performed immunostaining to detect fibrillarin, a nucleolar marker. We found that nucleoli were undetectable in pole cells at stage 4–5 (Figures 1A and 1E), at a time when they were observed in all somatic nuclei (Figure 1A). In pole cells, nucleoli began to form at stage 6–7 (Figures 1B and E) and became detectable in almost all pole cells by stage 8–9 (Figure 1E). This is compatible with the observations that pre-rRNA transcription can be faintly observed in newly formed pole cells at stage 4 and is subsequently upregulated in these cells at stage 5 (Seydoux and Dunn, 1997), whereas it is detected in all somatic nuclei from stage 4 onward (Falahati

et al., 2016; Seydoux and Dunn, 1997). Thus, nucleolar formation is delayed in pole cells relative to somatic cells and is initiated following pre-rRNA transcription.

Next, we sought to determine how nucleolar formation is delayed in pole cells. Given the transient absence of nucleoli in newly formed pole cells, we expected that nucleolar formation is repressed by a maternal factor that is partitioned into pole cells and then degraded rapidly in these cells. Maternal *pgc* mRNA is localized in pole plasm to produce the Pgc peptide only in pole cells (Hanyu-Nakamura et al., 2008; Martinho et al., 2004). Pgc peptide remains detectable until stage 5 but rapidly disappears by stage 6 (Hanyu-Nakamura et al., 2008), when nucleolar formation initiates (Figure 1E). As expected, in pole cells lacking maternal *pgc* (*pgc*$^{-}$ pole cells), nucleolar formation occurred at stage 4, substantially earlier than in normal (*y w*) pole cells (Figures 1C–1E). This observation shows that maternal *pgc* inhibits nucleolar formation in newly formed pole cells. Because the Pgc peptide represses RNA polymerase II (RNAP-II) activity in early pole cells (Hanyu-Nakamura et al., 2008; Martinho et al., 2004), we assume that RNAP-II-dependent transcription is required to initiate nucleolar formation in pole cells.

Because the nucleolus is the site of ribosome biogenesis, it is plausible that protein synthesis is lower in early pole cells lacking nucleoli relative to that in somatic cells. However, this is not the case: uptake of radioactive amino acids is higher in pole cells than in the somatic region (Zalokar, 1976); the higher rate of translation in pole cells is presumably due to maternally contributed ribosomes.

We noted that the microRNA gene *mir-10404* is encoded within the NOR of the nuclear genome, which encodes rRNAs (Chak et al., 2015). The hairpin sequence for *mir-10404* is located in the internal transcribed spacer 1 region (ITS1) of the NOR (Figure 1F) and is highly conserved among Dipteran species (Chak et al., 2015). miR-10404 expression was significantly elevated in *pgc*$^{-}$ pole cells but not in *pgc*$^{-}$ whole embryos (Figure 1G). This observation indicates that miR-10404 expression, as well as nucleolar formation, is repressed in newly formed pole cells by maternal *pgc*.

Repression of miR-10404 Expression Stabilizes *dap* mRNA in Pole Cells

Luciferase assays using cultured cells have revealed that miR-10404 can act *in trans* to downregulate expression of a reporter mRNA carrying its target sequence (Chak et al., 2015); however, the endogenous targets of miR-10404-dependent repression have remained elusive. To identify the endogenous targets, we identified 223 transcripts whose 3′ UTRs contain a sequence complementary to the miR-10404 seed sequence using TargetScanFly (www.targetscan.org) (Table S2); microRNAs degrade their targets by binding to their 3′ UTRs (Brennecke et al., 2005; Kim et al., 2017; Lai, 2002). Among the 223 transcripts, we selected *dacapo, red dog mine, Fmr1, β-Mannosidase, claret, raw,* and *abdominal A* as mRNAs whose levels were significantly reduced in *pgc*$^{-}$ pole cells (Table S3), as miR-10404 expression was derepressed in *pgc*$^{-}$ pole cells (Figure 1G). For further analysis, we focused on *dap*, which was more highly expressed than the other six transcripts in normal pole cells (Table S3). We found that, among the 223 transcripts, the expression of 206 was unaffected in *pgc*$^{-}$ pole cells and only 10 were up-regulated (Table S3). Because miR-10404 was repressed by *pgc* (Figure 1G), we did not consider these transcripts to be *bona fide* targets of miR-10404-dependent repression in pole cells.

dap mRNA is supplied maternally and is distributed throughout early cleavage embryos (stage 1–2) (Lane et al., 1996) (Figures 2A and 2A′). Prior to pole cell formation, *dap* mRNA is rapidly degraded in the somatic region and is consequently enriched in pole cells (FlyBase; www.flybase.org) (Lane et al., 1996) (Figure 2B and B′). We found that *dap* mRNA remained detectable in pole cells during stage 4–6 (Figures 2B–D and 2B′–2D′), but its expression decreased in these cells after stage 7 (Figures 2E, 2E′, 2F, and 2F′). Consequently, only a weak signal was detected in pole cells at stage 9 (Figures 2G and 2G′). By contrast, in *pgc*$^{-}$ pole cells, the *dap* mRNA signal rapidly decreased at stage 4–6 (Figures 2H–2K and 2H′–2K′), and the signal was no longer discernible in these cells after stage 7 (Figures 2L–2N and 2L′–2N′). These data show that *pgc* is required to stabilize maternal *dap* mRNA in early pole cells.

Considering that *dap* is a potential target of miR-10404-dependent RNA degradation, we expected that maternal *pgc* would repress expression of miR-10404, which would otherwise induce degradation of *dap* mRNA in early pole cells. To test this idea, we microinjected miR-10404 into the posterior pole of cleavage embryos at stage 1–2 [I(miR10404) embryos]. The maternal *dap* mRNA signal decreased rapidly in pole cells of I(miR10404) embryos (Figures 2S, 2S′, 2T, and 2T′), compared with that in pole cells of control embryos

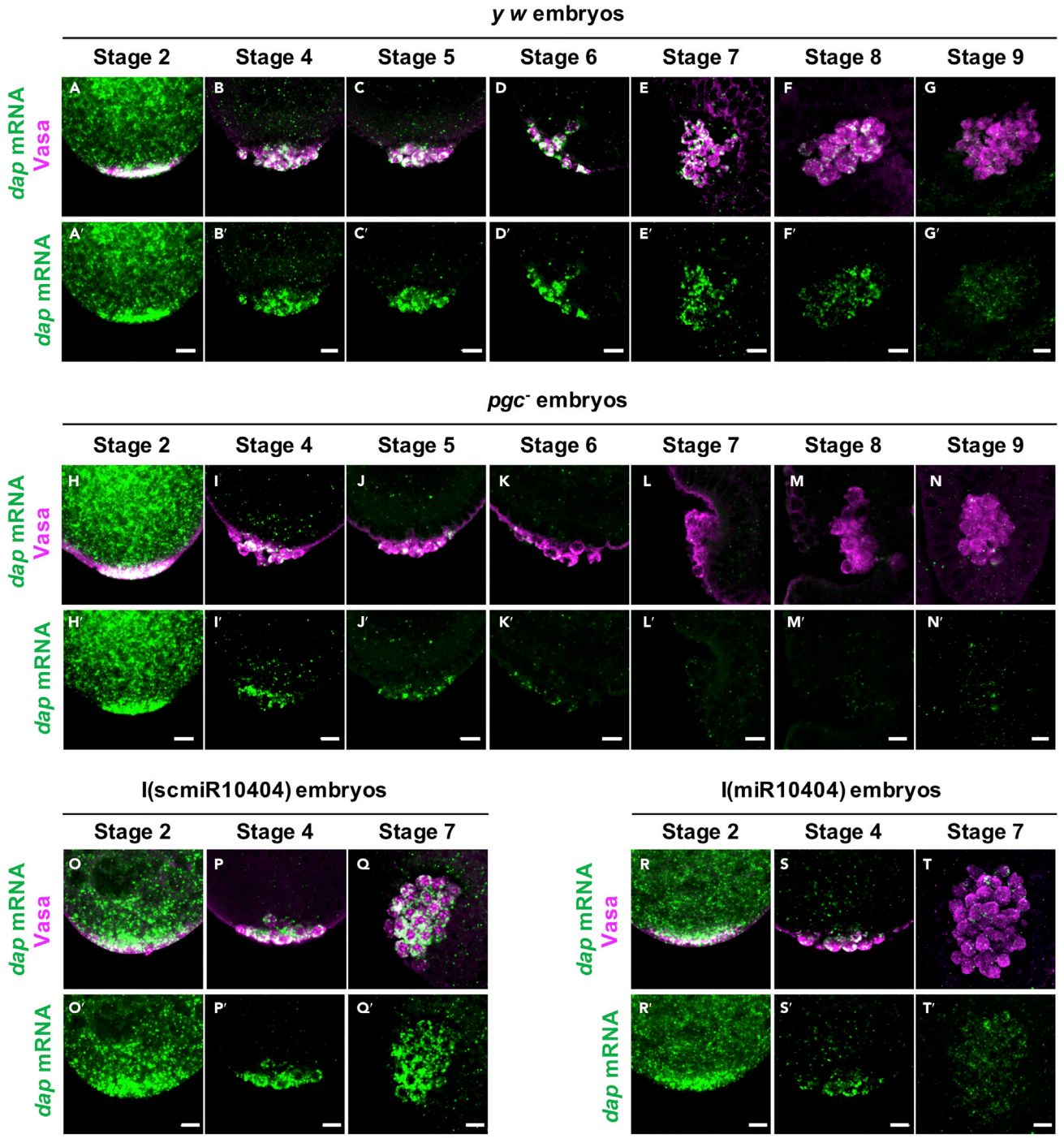

Figure 2. Degradation of Maternal *dap* mRNA Is Accelerated in *pgc*⁻ Pole Cells and in Pole Cells of Normal Embryos Injected with miR-10404

(A–N and A′–N′) Stage 2 (A, A′, H, and H′), stage 4 (B, B′, I, and I′), stage 5 (C, C′, J, and J′), stage 6 (D, D′, K, and K′), stage 7 (E, E′, L, and L′), stage 8 (F, F′, M, and M′), and stage 9 (G, G′, N, and N′) embryos derived from *y w* (*y w* embryos; A–G and A′–G′) and $pgc^{Δ1}/Df(2R)X58\text{-}7$ females (pgc^{-} embryos; H–N and H′–N′) were *in situ* hybridized with an RNA probe for *dap* mRNA (green) and immunostained for Vasa (magenta). Pole plasm (A, A′, H, and H′) and pole cells (B–G, B′–G′, I–N, and I′–N′) are shown. Scale bars: 10 μm.

(O–T and O′–T′) Stage 2 (O, O′, R, and R′), stage 4 (P, P′, S, and S′), and stage 7 embryos (Q, Q′, T, and T′) injected with scrambled miR-10404 [l(scmiR) embryos; O–Q and O′–Q′] and miR-10404 [l(miR) embryos; R–T and R′–T′] were *in situ* hybridized with an RNA probe for *dap* mRNA (green) and immunostained for Vasa (magenta). Pole plasm (O, O′, R, and R′) and pole cells (P, Q, P′, Q′, S, T, S′, and T′) are shown. Scale bars: 10 μm.

injected with a scrambled miR-10404 [I(scmiR10404) embryos] (Figures 2P, 2P′, 2Q, and 2Q′), although the signal was localized in the pole plasm of I(miR10404) and I(scmiR10404) embryos (Figures 2O, 2O′, 2R, and 2R′). These observations show that miR-10404 degrades *dap* mRNA in pole cells. Therefore, we conclude that *pgc*-dependent suppression of miR-10404 expression delays degradation of maternal *dap* mRNA in pole cells, which in turn allows its translation in these cells. Indeed, Dap protein accumulates to high levels in pole cells during gastrulation (De Nooij et al., 1996).

Suppression of miR-10404 Expression Inhibits G1/S Transition in Pole Cells by Stabilizing *dap* mRNA

Because Dap is a member of the p21/p27 family of Cdk inhibitors that blocks the G1/S transition by inhibiting the activity of Cyclin E-Cdk2 complex (Lane et al., 1996; De Nooij et al., 1996), it is possible that suppression of miR-10404 inhibits the G1/S transition in normal pole cells by stabilizing *dap* mRNA. However, we cannot test this idea by supplying miR-10404 to normal pole cells, because normal pole cells are arrested in G2 owing to the lack of Cyclin B (CycB) protein (Asaoka-Taguchi et al., 1999). To overcome this problem, we used embryos expressing CycB in pole cells. In these embryos, the pole cells are arrested in G1 after mitosis (Asaoka-Taguchi et al., 1999; Su et al., 1998). We mis-expressed *CycB* mRNA during oogenesis under the control of the *maternal-Gal4* driver. Replacement of the 3′ UTR of *CycB* mRNA with the *nos* 3′ UTR caused maternal *CycB* mRNA to localize to the pole plasm, where it was translated to produce CycB protein in pole cells (CycB embryos) (Figures S1A–S1F and S1A′–S1F′). These pole cells, but not normal ones, expressed a mitotic marker, a phosphorylated form of histone H3 (PH3), confirming that CycB-expressing pole cells entered mitosis (Figures S1G, S1G′, S1H, and S1H′).

We next asked whether supplying miR-10404 into pole cells would promote their transition from G1 to S in CycB embryos. When miR-10404 was injected into the posterior of CycB embryos [CycB-I(miR10404) embryos], pole cells were labeled with 5-ethynyl-2′-deoxyuridine (EdU) (Figures 3B and 3D), whereas no EdU-labeled pole cells were detectable in CycB embryos injected with scrambled miR-10404 [CycB-I(scmiR10404) embryos] (Figures 3A and 3D). This observation shows that miR-10404 promotes the G1/S transition in pole cells.

Because *dap* mRNA is a target for miR-10404-dependent degradation in pole cells (Figures 2S, 2S′, 2T, and 2T′), we expected that derepression of the G1/S transition caused by injection of miR-10404 can be rescued by supplying *dap* mRNA into pole cells. When *dap* mRNA, in which the 5′ and 3′ UTRs were replaced by the corresponding regions from *nos* mRNA, was co-injected with miR-10404 into the posterior of CycB embryos [CycB-I(miR10404+*dap*) embryos], the percentage of EdU-labeled pole cells was significantly lower than in CycB-I(miR10404) embryos (Figures 3C and 3D). These results show that derepression of the G1/S transition in pole cells of CycB-I(miR10404) embryos is rescued by supplying *dap* mRNA. Therefore, we propose that suppression of miR-10404 inhibits the G1/S transition in normal pole cells by stabilizing *dap* mRNA.

The above observations raise the question of whether miR-10404 degrades *dap* mRNA directly. This could be tested by deleting the miR-10404-binding site on *dap* mRNA and examining its effect on G1/S transition in pole cells of CycB-I(miR10404) embryos. Another question is whether miR-10404-dependent cell-cycle regulation through *dap* mRNA degradation is seen in cell types other than pole cells. Although the cell types expressing both miR-10404 and *dap* mRNA remain unclear, we favor the idea that mature miR-10404 is not necessarily produced in all (or almost all) somatic cells with prominent nucleoli. This is based on the fact that mature miR-10404 is produced by a noncanonical miRNA processing pathway that bypasses cleavage by the Drosha/Pasha complex but requires the Dcr-1/loqs complex (Chak et al., 2015), suggesting that miR-10404 is produced in a cell type- and/or stage-specific manner. Future studies are needed to identify the cell types that express both miR-10404 and *dap* mRNA and to test whether miR-10404 overexpression enhances S-phase entry, thereby repressing *dap* expression in these cells.

Derepression of the G1/S Transition Causes Defects in Pole Cell Maintenance and Pole Cell Migration

Proper migration of pole cells into the gonads is unaffected by either mis-expression of CycB or the resultant single round of mitosis (Asaoka-Taguchi et al., 1999). Hence, we asked whether the G1/S transition in pole cells of CycB-I(miR10404) embryos affects proper pole cell migration during embryogenesis. In CycB-I(miR10404) embryos, the number of pole cells within the gonads was significantly reduced, and conversely, pole cell number outside the gonads was elevated, compared with CycB-I(scmiR10404) embryos (Figure 3E). Furthermore, we found that the total number of pole cells within an embryo (no. of pole cells

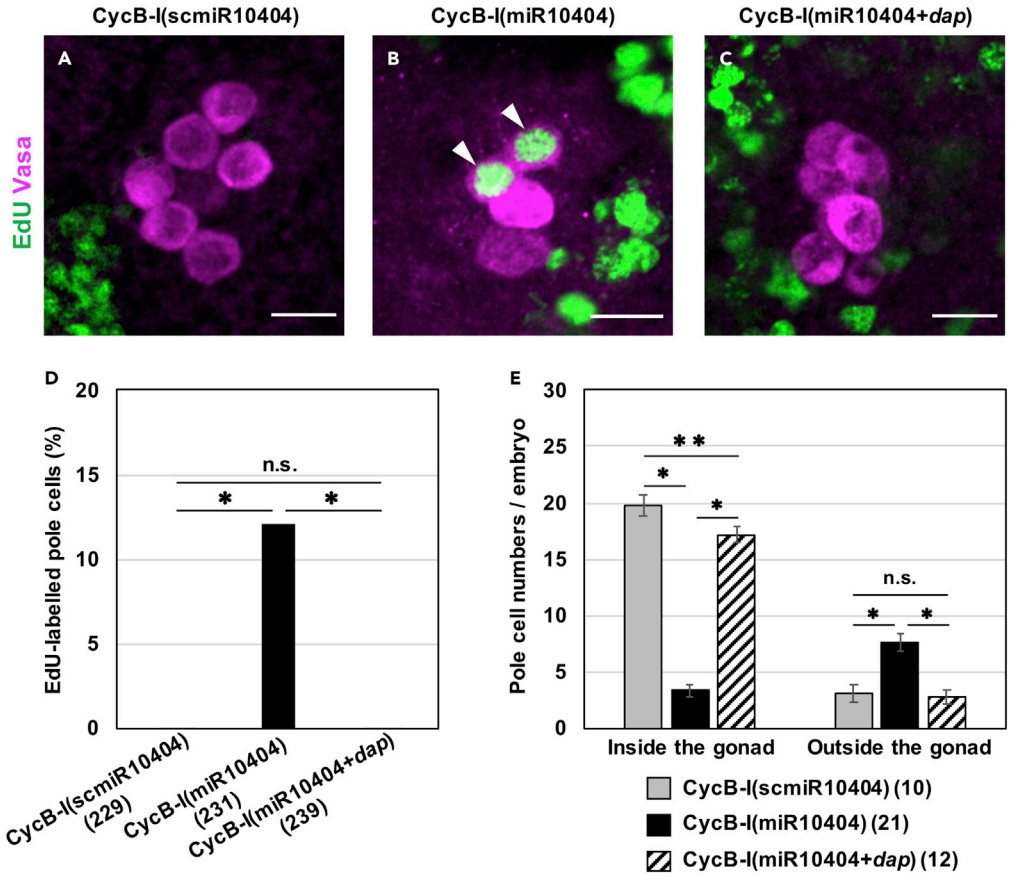

Figure 3. Derepression of the G1/S Transition in Pole Cells of CycB Embryos Injected with miR-10404 and Defects in Their Maintenance and Their Migration into the Gonads

(A–C) Pole cells in a CycB-I(scmiR10404) embryo (A), a CycB-I(miR10404) embryo (B), and a CycB-I(miR10404+*dap*) embryo (C) at stage 15 were stained for EdU (green) and immunostained for Vasa (magenta). EdU was incorporated into the nuclei of pole cells within embryos (B). White arrowheads indicate EdU-labeled pole cells. Scale bars: 10 μm.

(D) Percentage of EdU-labeled pole cells in CycB-I(scmiR10404), CycB-I(miR10404), and CycB-I(miR10404+*dap*) embryos. The numbers of pole cells examined are shown in parentheses. Significance was calculated by Fisher's exact test (*: $p < 0.01$, n.s.: $p > 0.05$).

(E) Average number of pole cells within and outside the gonad in CycB-I(scmiR10404) (shaded bars), CycB-I(miR10404) (solid bars), and CycB-I(miR10404+*dap*) embryos (hatched bars), which were developing normally to stage 13–15. Numbers of embryos examined are shown in parentheses. Significance was calculated by Student's t test (*: $p < 0.01$, **: $0.01 < p < 0.05$, n.s.: $p > 0.05$). The total number of pole cells within an embryo was also reduced in CycB-I(miR10404) embryos (the average number of pole cells [AN] ± standard error [SE] = 11 ± 0.78 [Student's t test, $p < 0.01$]), compared with CycB-I(scmiR10404) (AN ± SE = 22.9 ± 1.26) and CycB-I(miR10404+*dap*) embryos (AN ± SE = 19.9 ± 0.80).

inside + outside gonads) was also significantly reduced in CycB-I(miR10404) embryos relative to CycB-I(scmiR10404) embryos (see the legend for Figure 3E). Moreover, the decrease in the total number of pole cells and the inability of pole cells to migrate into the gonads were rescued by injecting *dap* mRNA in CycB-I(miR10404) embryos (Figure 3E). Since the pole cell defects were almost fully rescued by *dap* alone (Figure 3E), the rest of the six downstream candidates for miR-10404 in pole cells (Table S2) have limited, if any, contribution to pole cell development in embryos. Based on these data, we propose that repression of the G1/S transition, which results from *dap* stabilization due to the absence of miR-10404, is required in pole cells for their maintenance and migration into the embryonic gonads.

Cell-Cycle Regulation in Pole Cells

In *Drosophila*, Nos protein produced from maternal *nos* mRNA inhibits the G2/M transition in pole cells by suppressing translation of maternal *CycB* mRNA (Asaoka-Taguchi et al., 1999). Premature mitosis

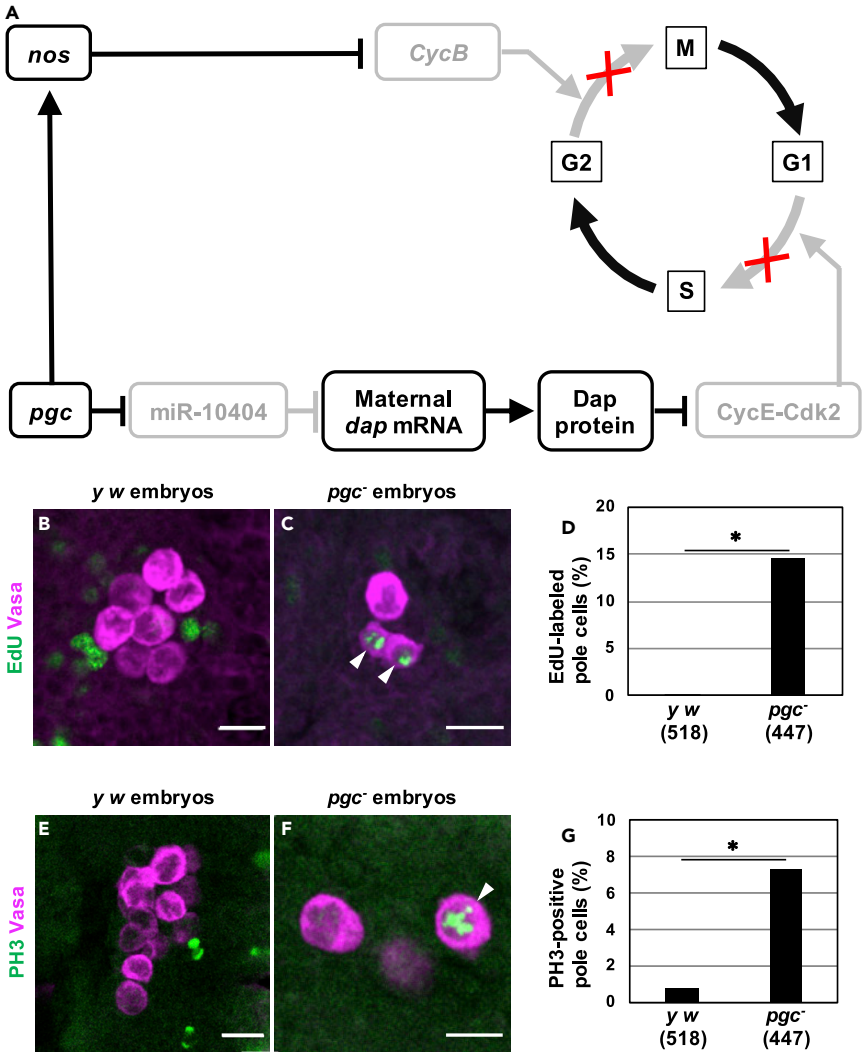

Figure 4. A Model Explaining Cell-Cycle Quiescence in Pole Cells, and Derepression of Cell-Cycle Quiescence in *pgc*⁻ Pole Cells

(A) Maternal *pgc* represses miR-10404 expression in stage 4 and stage 5 pole cells. Repression of miR-10404 expression delays the degradation of maternal *dap* mRNA to produce Dap protein in pole cells. Dap protein prevents the CycE-Cdk2 complex to block the G1/S transition. On the other hand, maternal *pgc* is also required in pole cells to stabilize maternal *nos* mRNA. Nos protein produced from maternal *nos* mRNA represses the translation of CycB to block the G2/M transition. Consequently, the G2/M and G1/S transition are both blocked in normal pole cells.

(B and C) Pole cells in *y w* (B) and *pgc*⁻ embryos (C) at stage 15 were stained for EdU (green) and immunostained for Vasa (magenta). EdU was incorporated in the nuclei of pole cells in *pgc*⁻ (C) embryos. White arrowheads indicate EdU-positive pole cells. Scale bars: 10 μm.

(D) Percentage of EdU-labeled pole cells in *y w* and *pgc*⁻ embryos. Numbers of pole cells examined are shown in parentheses. Significance was calculated between *y w* and *pgc*⁻ by Fisher's exact test (*: $p < 0.05$).

(E and F) Pole cells in *y w* (E) and *pgc*⁻ (F) embryos at stage 13–15 were immunostained for PH3 (green) and Vasa (magenta). PH3 was expressed in the nuclei of pole cells within *pgc*⁻ embryos (F). White arrowheads indicate PH3-positive pole cells. Scale bars: 10 μm.

(G) Percentage of PH3-positive pole cells in *y w* and *pgc*⁻ embryos. Numbers of pole cells examined are shown in parentheses. Significance was calculated between *y w* and *pgc*⁻ by Fisher's exact test (*: $p < 0.05$).

induced by the lack of maternal *nos* activity or CycB mis-expression is never followed by the S phase (Asaoka-Taguchi et al., 1999; Su et al., 1998), indicating that the G1/S transition is also inhibited in pole cells. Here, we provide evidence that, in normal pole cells, *pgc*-dependent

suppression of miR-10404 expression delays the degradation of *dap* mRNA, repressing the G1/S transition (Figure 4A).

pgc^{-} pole cells exhibit premature loss of maternal *nos* mRNA (Deshpande et al., 2012; Hanyu-Nakamura et al., 2019), and CycB protein production is derepressed in *pgc*$^{-}$ pole cells owing to the absence of Nos-dependent translational repression of maternal *CycB* mRNA (Deshpande et al., 2012). In combination with our data, these observations suggest that depletion of maternal *pgc* alone causes derepression of both the G2/M and G1/S transitions in pole cells (Figure 4A). We found that this is the case; EdU labeling and PH3 expression were both evident in *pgc*$^{-}$ pole cells but not in normal (*y w*) embryos (Figures 4B–4G). These phenotypes were compatible with those observed in CycB-I(miR10404) embryos (Figures 3B and 3D).

Moreover, a decrease in the total number of pole cells and an alteration in the ability of pole cells to migrate into embryonic gonads were evident in CycB-I(miR10404) embryos but not in CycB-I(scmiR10404) embryos (Figure 3E). This suggests that the G1/S transition, but not the G2/M transition, causes defects in pole cell maintenance and pole cell migration, although it remains unknown how the G1/S transition leads to these abnormalities. One possible explanation for this is that the G1/S transition may alter histone modifications in pole cells. In the soma of *Drosophila* embryos, active (H3K4me3) and repressive (H3K27me3) modifications of histone H3 are replaced by unmethylated histone H3 following DNA replication (Petruk et al., 2012). Consequently, these modifications are reduced through the S phase but are re-established in the soma by histone-modifying enzymes, thereby maintaining the histone code (Xu et al., 2012). Thus, it is possible that the aberrant DNA replication in early pole cells may cause erasure of chromatin modifications, due to the lack of machinery capable of restoring the normal histone marks. This erasure of histone modifications may alter gene expression in pole cells, which in turn results in their failure to follow proper germline development. Another possible mechanism is that derepression of both the G2/M and G1/S transition, but not the G2/M transition alone, could induce multiple rounds of mitosis in pole cells, resulting in the dilution of regulatory proteins involved in modulating downstream gene expression and/or germline-specific cellular function. Thus, repression of both the G2/M and G1/S transition is required in pole cells to keep the cellular concentration of such proteins high enough for their proper function.

Our observations indicate that the delay in miR-10404 expression is necessary to repress the G1/S transition in early pole cells. Furthermore, our previous observation shows that inhibition of CycB production represses the G2/M transition in pole cells (Asaoka-Taguchi et al., 1999). These two series of studies indicate that continued cell cycling of pole cells is tightly blocked through multiple cell-cycle checkpoints. Moreover, we found that repression of the G1/S transition is required in pole cells for their proper maintenance and migration into embryonic gonads. Our findings raise questions for future studies: (1) Does derepression of cell cycling alter expression of the genes required for germline development in pole cells? (2) To what extent does cell-cycle quiescence of germline progenitors play conserved roles in proper gamete development in animals? Cell-cycle quiescence has been observed in the germline of sea urchin, frog, nematode, mouse, and fruit fly (Asaoka-Taguchi et al., 1999; Fukuyama et al., 2006; Juliano et al., 2010; Kalt and Joseph, 1974; Nakamura and Seydoux, 2008; Seki et al., 2007; Su et al., 1998). Thus, our findings clarify the widespread role of cell-cycle quiescence in germline development.

Limitations of the Study

Here, we showed that *pgc*-dependent suppression of miR-10404 expression delays the degradation of *dap* mRNA, repressing G1/S transition in normal pole cells. However, we did not examine experimentally whether miR-10404 degrades *dap* mRNA via direct binding to the *dap* 3′ UTR and whether repression of G1/S transition is relevant to germline development even in the presence of G2/M arrest. Furthermore, it remains unclear whether miR-10404-dependent cell-cycle regulation through *dap* mRNA degradation occurs in cell types other than pole cells. Future studies should seek to clarify these issues.

METHODS

All methods can be found in the accompanying Transparent Methods supplemental file.

DATA AND CODE AVAILABILITY

The accession number for the all RNA-seq data reported in this paper is DNA Data Bank of Japan (DDBJ): DRA009066.

SUPPLEMENTAL INFORMATION

Supplemental Information can be found online at https://doi.org/10.1016/j.isci.2020.100950.

ACKNOWLEDGMENTS

We thank Dr. Akira Nakamura for providing us with *pgc*$^{\Delta}$*1*/*CyO* flies. We also thank the Genomics Center of University of Minnesota for Illumina next-generation sequencing, the Bloomington Drosophila Stock Center for providing us with fly stocks, and the Developmental Studies Hybridoma Bank for antibodies. This work was supported in part by Grants-in-Aid for Scientific Research from the Japan Society for the Promotion of Science, Japan (JSPS) (KAKENHI Grant Numbers: 25114002 and 18H05552) We thank members of the Kobayashi laboratory for valuable discussions.

AUTHOR CONTRIBUTIONS

S.M. and S.K. designed the experiments. S.M., R.O., and M.H. performed the experiments, and S.M. performed bioinformatics analysis. S.M. and S.K. wrote the paper. All authors reviewed the manuscript.

DECLARATION OF INTERESTS

The authors declare no competing interests.

Received: November 25, 2019
Revised: January 20, 2020
Accepted: February 24, 2020
Published: March 27, 2020

REFERENCES

Asaoka-Taguchi, M., Yamada, M., Nakamura, A., Hanyu, K., and Kobayashi, S. (1999). Maternal Pumilio acts together with Nanos in germline development in *Drosophila* embryos. Nat. Cell Biol. *1*, 431–437.

Brennecke, J., Stark, A., Russell, R.B., and Cohen, S.M. (2005). Principles of MicroRNA-target recognition. PLoS Biol. *3*, 0404–0418.

Chak, L., Mohammed, J., Lai, E.C., Tucker-Kellogg, G., and Okamura, K. (2015). A deeply conserved, noncanonical miRNA hosted by ribosomal DNA. RNA *21*, 375–384.

Deshpande, G., Spady, E., Goodhouse, J., and Schedl, P. (2012). Maintaining sufficient nanos is a critical function for *Polar Granule Component* in the specification of primordial germ cells. G3 (Bethesda) *2*, 1397–1403.

Falahati, H., Pelham-Webb, B., Blythe, S., and Wieschaus, E. (2016). Nucleation by rRNA dictates the precision of nucleolus assembly. Curr. Biol. *26*, 277–285.

Fukuyama, M., Rougvie, A.E., and Rothman, J.H. (2006). *C. elegans* DAF-18/PTEN mediates nutrient-dependent arrest of cell cycle and growth in the germline. Curr. Biol. *16*, 773–779.

Hanyu-Nakamura, K., Sonobe-Nojima, H., Tanigawa, A., Lasko, P., and Nakamura, A. (2008). *Drosophila* Pgc protein inhibits P-TEFb recruitment to chromatin in primordial germ cells. Nature *451*, 730–733.

Hanyu-Nakamura, K., Matsuda, K., Cohen, S.M., and Nakamura, A. (2019). Pgc suppresses the zygotically acting RNA decay pathway to protect germ plasm RNAs in the *Drosophila* embryo. Development *146*, dev167056.

Illmensee, K., and Mahowald, A.P. (1974). Transplantation of posterior polar plasm in *Drosophila*. Induction of germ cells at the anterior pole of the egg. Proc. Natl. Acad. Sci. U S A *71*, 1016–1020.

Juliano, C.E., Yajima, M., and Wessel, G.M. (2010). Nanos functions to maintain the fate of the small micromere lineage in the sea urchin embryo. Dev. Biol. *337*, 220–232.

Kadyrova, L.Y., Habara, Y., Lee, T.H., and Wharton, R.P. (2007). Translational control of maternal *Cyclin B* mRNA by Nanos in the *Drosophila* germline. Development *134*, 1519–1527.

Kalt, M.R., and Joseph, G.G. (1974). Observations ON early germ cell development and premeiotic ribosomal DNA amplification IN *XENOPUS LAEVIS*. J. Cell Biol. *62*, 460–472.

Kim, D., Chang, H.R., and Baek, D. (2017). Rules for functional microRNA targeting. BMB Rep. *50*, 554–559.

Lai, E.C. (2002). Micro RNAs are complementary to 3′ UTR sequence motifs that mediate negative post-transcriptional regulation. Nat. Genet. *30*, 363–364.

Lane, M.E., Sauer, K., Wallace, K., Jan, Y.N., Lehner, C.F., and Vaessin, H. (1996). Dacapo, a cyclin-dependent kinase inhibitor, stops cell proliferation during *Drosophila* development. Cell *87*, 1225–1235.

Mahowald, A.P. (1968). Polar granules of *Drosophila* II. ultrastructual changes during early embryogenesis. J. Exp. Zool. *167*, 237–262.

Martinho, R.G., Kunwar, P.S., Casanova, J., and Lehmann, R. (2004). A noncoding RNA is required for the repression of RNApolII-dependent transcription in primordial germ cells. Curr. Biol. *14*, 159–165.

Nakamura, A., and Seydoux, G. (2008). Less is more: specification of the germline by transcriptional repression. Development *135*, 3817–3827.

De Nooij, J.C., Letendre, M.A., and Hariharan, I.K. (1996). A cyclin-dependent kinase inhibitor, dacapo, is necessary for timely exit from the cell cycle during *Drosophila* embryogenesis. Cell *87*, 1237–1247.

Petruk, S., Sedkov, Y., Johnston, D.M., Hodgson, J.W., Black, K.L., Kovermann, S.K., Beck, S., Canaani, E., Brock, H.W., and Mazo, A. (2012). TrxG and PcG proteins but not methylated histones remain associated with DNA through replication. Cell *150*, 922–933.

Richardson, B.E., and Lehmann, R. (2010). Mechanisms guiding primordial germ cell migration: Strategies from different organisms. Nat. Rev. Mol. Cell Biol. *11*, 37–49.

Seki, Y., Yamaji, M., Yabuta, Y., Sano, M., Shigeta, M., Matsui, Y., Saga, Y., Tachibana, M., Shinkai, Y., and Saitou, M. (2007). Cellular dynamics associated with the genome-wide epigenetic reprogramming in migrating primordial germ cells in mice. Development *134*, 2627–2638.

Seydoux, G., and Dunn, M.A. (1997). Transcriptionally repressed germ cells lack a subpopulation of phosphorylated RNA polymerase II in early embryos of *Caenorhabditis elegans* and *Drosophila melanogaster*. Development *124*, 2191–2201.

Sonnenblick, B.P. (1941). Germ cell movements and sex differentiation of the gonads in the *Drosophila* embryo. Proc. Natl. Acad. Sci. U S A *27*, 484–489.

Su, T.T., Campbell, S.D., and O'Farrell, P.H. (1998). The cell cycle program in germ cells of the *Drosophila* embryo. Dev. Biol. *196*, 160–170.

Technau, G.M., and Campos-Ortega, J.A. (1986). Lineage analysis of transplanted individual cells in embryos of *Drosophila melanogaster*. Roux's Arch. Dev. Biol. *195*, 389–398.

Underwood, E.M., Caulton, J.H., Allis, C.D., and Mahowald, A.P. (1980). Developmental fate of pole cells in *Drosophila melanogaster*. Dev. Biol. *77*, 303–314.

Xu, M., Wang, W., Chen, S., and Zhu, B. (2012). A model for mitotic inheritance of histone lysine methylation. EMBO Rep. *13*, 60–67.

Zalokar, M. (1976). Autoradiographic study of protein and RNA formation during early development of *Drosophila* eggs. Dev. Biol. *49*, 425–437.

iScience, Volume *23*

Supplemental Information

Repression of G1/S Transition by Transient Inhibition of miR-10404 Expression in *Drosophila* Primordial Germ Cells

Shumpei Morita, Ryoma Ota, Makoto Hayashi, and Satoru Kobayashi

Supplemental Information

Transparent Methods

Flies

Flies were maintained on standard *Drosophila* medium at 25 °C. *y w* was used as the normal strain, *matα4-GAL-VP16* (*maternal-Gal4*) (Stock No. 7063), *y1 M{vas-int.Dm}ZH-2A w*; *M{3xP3-RFP.attP'}ZH-86Fa* (24486), and *Df(2R)X58-7*/*CyO* (283) were provided by the Bloomington Drosophila Stock Center. *pgcΔ1*/*CyO* was a gift from Dr. Akira Nakamura.

Transgenes

For construction of pUASp-CycB-nos3′ UTR, total RNA was isolated from early embryos using ISOGEN (NIPPON GENE, Cat#311-02501), and cDNA was synthesized using SuperScript III Reverse Transcriptase (Thermo Fisher Scientific, Cat#18080093). The open reading frame (ORF) of *CycB* was amplified from the cDNA using primer pair Fw-CycB-ORF/Rv-CycB-ORF (Table S1). The *nos* 3′-UTR was amplified from *NdeI*-digested pBS-Pnos-nos3'UT (Asaoka-Taguchi et al., 1999) using primer pair Fw-nos3′ UTR/Rv-nos3′ UTR (Table S1). The *CycB* ORF and *nos* 3′ UTR were cloned into *Kpn*I/*Not*I-digested pUASp-K10-attB vector (Koch et al., 2009) using Gibson Assembly (New England Biolabs, Cat#E2611L). Germline transformation was performed using *y1 M{vas-int.Dm}ZH-2A w*; *M{3xP3-RFP.attP'}ZH-86Fa* embryos as recipients using the *Φ*C31 integrase-mediated transgenesis system (Bischof et al., 2007). *w+* transformants were crossed to *w*; *sp*/*CyO*; *PrDr*/*TM3* females to establish homozygous stocks.

Fixation of embryos

Embryos were dechorionated in a sodium hypochlorite solution. The dechorionized embryos were washed with distilled water (DW) and fixed for 30 min in 1:1 heptane:fixative [4% paraformaldehyde in PBS (130 mM NaCl, 7 mM Na_2HPO_4, and 3 mM NaH_2PO_4)]. Vitelline membrane of fixed embryos was removed in 1:1 methanol:heptane by vigorous shaking. Vitelline membranes of injected embryos were removed manually. The embryos were then washed with PBST (0.1% Tween20 and 0.1% Triton-X100 in PBS) three times for 20 min each.

Immunostaining

The fixed and devitellinized embryos were incubated in blocking solution (2% BSA in PBST) for 30 min. After blocking, the embryos were incubated in the following primary antibodies overnight at 4℃ with the indicated dilutions: rabbit anti-fibrillarin (1:500) (abcam, Cat#ab5821), chick anti-Vasa (1:500) (Hayashi et al., 2017), rabbit anti-phospho histone H3 (1:500) (Millipore, Cat#06-570), and mouse anti-CycB (1:10) (Developmental Studies Hybridoma Bank, DSHB: F2F4). Then, the embryos were washed with PBST three times for 20 min each. For detection of primary antibodies, the following secondary antibodies were used: Alexa Fluor 488–conjugated goat anti-rabbit (1:500) (Molecular Probe, Cat#A-11034), Alexa Fluor 488–conjugated goat anti-mouse (1:500) (Molecular Probe, Cat#A-11029), Alexa Fluor 546–conjugated goat anti-chick (1:500) (Molecular Probe, Cat#A-11030), and Alexa Fluor 633–conjugated goat anti-rabbit (1:500) (Molecular Probe, Cat#A-21071). The embryos were washed with PBST three times for 20 min each, and then mounted in ProLong Diamond Antifade Mountant (Thermo Fisher Scientific, Cat#P36961). The embryos were observed by confocal microscopy SP5 (Leica Microsystems). The number of pole cells was counted using the Fiji software (Schindelin et al., 2012)

***In situ* hybridization**

The fixed and devitellinized embryos were rinsed with ME [50 mM EGTA (pH 8.0) in 90% methanol] and incubated in 7:3, 5:5, and 3:7 ME:fixative for 5 min each. The embryos were then incubated in fixative for 20 min and washed three times with PBST. They were then incubated for 3 min in 50 µg/ml Proteinase K in PBST. The digestion was stopped by incubation for 20 min in fixative, followed by three washes for 10 min each in PBST. The re-fixed embryos were incubated with Pre-HS [50% formamide, 5 x SSC (1 x SSC is 150 mM NaCl and 15 mM sodium-citrate), 100 µg/ml heparin, 100 µg/ml yeast tRNA, 10 mM DTT, and 0.1% Tween20] for 1 h at 60 °C, and then hybridized with 2 ng/µl of RNA probe in HS (10% dextran sulfate in Pre-HS) overnight at 60 °C. After hybridization, the embryos were washed six times at 60 °C in a solution containing 50% formamide, 5 x SSC, and 0.1% Tween 20. Signal was detected using anti-Digoxigenin-POD antibody (Roche, Cat#11633716001) and amplified using TSA Biotin System and Streptavidin–Fluorescein Isothiocyanate Conjugate (PerkinElmer, Cat#NEL700A001KT). Samples were mounted in ProLong Diamond Antifade Mountant (Thermo Fisher Scientific, Cat#P36961) and observed on an SP5 confocal microscope (Leica Microsystems).

To synthesize an RNA probe for *dap* mRNA, total RNA was isolated from embryos using ISOGEN (NIPPON GENE, Cat#311-02501), and cDNA was synthesized using SuperScript III Reverse Transcriptase (Thermo Fisher Scientific, Cat#18080093). The cDNA corresponding to *dap* was PCR-amplified using a primer pair containing T7 and T3 promoter sequence "Fw-dap-FISH/Rv-dap-FISH" (Table S1). Digoxigenin (DIG)-labeled RNA probes were synthesized with T7 or T3 RNA polymerase (Roche) using the fragment amplified by PCR.

5-ethynil-2´-deoxyuridine (EdU) labeling

EdU labeling was performed by using the Click-iT EdU Alexa Fluor 488 Imaging Kit (Thermo Fisher Scientific, Cat#C10337). Embryos at stage 15 were dechorionated in a sodium hypochlorite solution for 15 sec. To permeabilize the vitelline membrane, the embryos were incubated in DW-

saturated octane for 15 sec. The permeabilized embryos were incubated for 30 min in Grace's insect medium (Thermo Fisher Scientific, Cat#11605094) containing 200 µM Click-iT EdU (Thermo Fisher Scientific, Cat#C10337) with gentle shaking. After incubation, the embryos were fixed and devitellinized as described above (see Fixation of Embryos). For the Click-iT reaction, embryos were incubated in Click-iT reaction cocktail in the dark for 30 min, and then washed with PBST three times for 20 min each. When the embryos were double-stained for EdU and Vasa, the embryos were processed for immunostaining as described above (see Immunostaining) after the Click-iT reaction. Samples were mounted in ProLong Diamond Antifade Mountant (Thermo Fisher Scientific, Cat#P36961) and observed on an SP5 confocal microscope (Leica Microsystems).

RT-qPCR of miR-10404

Two hundred pole cells were collected by fluorescence-activated cell sorting (FACS) using *EGFP-vas* (Sano et al., 2002; Shigenobu et al., 2006) in a 0.2-ml PCR tube containing 2 µl RNase-free water (TaKaRa) at 4 °C in a PCR chill rack (IsoFreeze; Scientific Specialties, Inc.). Following centrifugation at 10,000 *g* for 1 min at 4 °C, the tube was shaken on a MixMate (Eppendorf) at 2000 rpm for 30 sec, and cDNA was synthesized from the lysate using the Mir-X miRNA First-Strand Synthesis Kit (Clontech, Cat#638313). Total RNA was extracted from whole embryos using the miRNeasy Mini Kit (QIAGEN, Cat#217004), and cDNA was synthesized from total RNA using the Mir-X miRNA First-Strand Synthesis Kit (Clontech, Cat#638313). From the pole cell and whole embryo cDNAs, miR-10404 and *ribosomal protein 49* (*rp49*) were amplified using primer pairs Fw-miR-10404/mRQ 3´ Primer and Fw-rp49/Rv-rp49 (Table S1), respectively. mRQ 3´ Primers were supplied by Clontech (Mir-X miRNA First-Strand Synthesis Kit). Quantifications were performed on a Light Cycler 480 system (Roche) with SYBR Advantage qPCR Premix (Clontech, Cat#638321). Data were analyzed using the LightCycler 480 Software (Roche) and

Microsoft Excel (Microsoft). Three independent experiments were carried out using different batches of flies.

Candidate targets for miR-10404

We identified transcripts whose 3´-UTRs contain nucleotide sequences complementary to the miR-10404 seed sequence using TargetScanFly (www.targetscan.org, release 6.2) (Table S1). The miR-10404 core seed is a six-nucleotide sequence beginning at position 2 from the 5´-end of the miRNA (Chak et al., 2015; Kim et al., 2017). To screen for candidate transcripts, we used seven nucleotides beginning at positions 1 (UAUUGAA) and 2 (AUUGAAG) from the 5´-end of miR-10404 as queries, both of which contain the core seed sequence (AUUGAA) (Table S2).

RNA-sequencing analysis of *pgc*- pole cells

Embryos produced from *pgc*$^{\Delta 1}$/*Df*(*2R*)*X58-7* ; *EGFP-vas* and *EGFP-vas* females were collected for 1 h, and then incubated for 2 h at 25 °C. One hundred pole cells were isolated from these embryos by FACS (Sano et al., 2002; Shigenobu et al., 2006). The pole cells were collected in a 0.2-ml PCR tube containing 10.5 µl of 1x reaction buffer (SMART-Seq v4 Ultra Low Input RNA Kit for Sequencing; Clontech, Cat#634890) at 4 °C in a PCR chill rack (IsoFreeze; Scientific Specialties, Inc.). Following centrifugation at 10,000 *g* for 1 min at 4 °C, the tube was shaken on a MixMate (Eppendorf) at 2000 rpm for 30 sec. cDNAs were synthesized from the pole cells using the SMART-Seq v4 Ultra Low Input RNA Kit for Sequencing (Clontech, Cat#634890). Nextera XT library creation and RNA-sequencing were carried out in University of Minnesota Genomics Center (UMGC) using the HiSeq 2500 platform (Illumina), and approximately 20 million reads per a sample (50-bp paired end reads) were obtained. Raw reads were processed using Trimmomatic, and then were pseudo-aligned to the *Drosophila* transcriptome (Flybase; dmel-all-transcript-r6.17.fasta) by using Kallisto (ver. 0.43.1) with default settings (Bray et al., 2016). Fold-

changes and p-values in *pgc*$^{\Delta 1}$/*Df(2R)X58-7* ; *EGFP-vas* pole cells relative to those in *EGFP-vas* pole cells were calculated using edgeR (Robinson et al., 2009). False discovery rate (FDR) was calculated by the Benjamini-Hochberg procedure, and transcripts with FDR values less than 0.05 were selected (Table S3). RNA-seq data were deposited in DDBJ under Accession No. DRA009066.

In vitro transcription

The *dap* coding region was amplified from an embryonic cDNA library (Brown and Kafatos, 1988) using primer pair Fw-Dap-nosUTR / Rv-Dap-nosUTR (Table S1). The EGFP coding region was amplified from pEGFP-N1 (Clontech, addgene: 6085-1) using primer pair Fw-EGFP-nosUTR / Rv-EGFP-nosUTR. These fragments were cloned into a unique *Nde*I site in pBS-Pnos-nos3'UT (Asaoka-Taguchi et al., 1999) to generate pBS-Pnos-dap-nos3´UT and pBS-Pnos-EGFP-nos3´UT, respectively. *nos5´UTR-dap-nos3´UTR* RNA (*dap* RNA) and *nos5´UTR-EGFP-nos3´UTR* RNA (*EGFP* RNA) were transcribed using the mMESSAGE mMACHINE T7 ULTRA Transcription Kit (Thermo Fisher Scientific, Cat#AM1345) from DNA fragments amplified using primer pair Fw-T7nos / Rv-nosUTR (Table S1) from pBS-Pnos-dap-nos3´UT and pBS-Pnos-EGFP-nos3´UT , respectively. These mRNAs were precipitated with lithium chloride and eluted with RNase free water.

Microinjection

Embryos produced from *y w* females were collected for 30 min at 25 °C. Each embryo was injected with 0.1 nl of 4.4 µg/µl miR-10404 (KOKEN, sequence: UAUUGAAGGAAUUGAUAUAUGC, miRbase: MIMAT0041637) [I(miR10404)], or 0.1 nl of 4.4 µg/µl scrambled miR-10404 (KOKEN, sequence: AUAUUGGUACUAGUGAUAGAUA) [I(scmiR10404)]. The injected embryos were

allowed to develop in a moist chamber for 0 h (stage 2), 2 h (stage 4), or 4 h (stage 7) at 18 °C, and were subsequently stained for *dap* mRNA and Vasa as described above.

Embryos derived from females with one copy each of *maternal-Gal4* and *UASp-CycB-nos3´UTR* (CycB embryos) were collected for 30 min at 25 °C. Each embryo was injected with 0.1 nl of 4.4 µg/µl miR-10404 (KOKEN) and 0.8 µg/µl *dap* RNA [CycB-I(miR10404+dap)], 0.1 nl of 4.4 µg/µl miR-10404 and 1.3 µg/µl *EGFP* RNA [CycB-I(miR10404)], or 0.1 nl of 4.4 µg/µl scrambled miR-10404 (KOKEN) and 1.3 µg/µl *EGFP* RNA [CycB-I(scmiR10404)]. The injected embryos were incubated in a moist chamber for 20 h at 18 °C, and processed for EdU labeling and immunostaining for Vasa.

Figure S1. CycB and PH3 expression in pole cells of CycB embryos. Related to Figure 3.

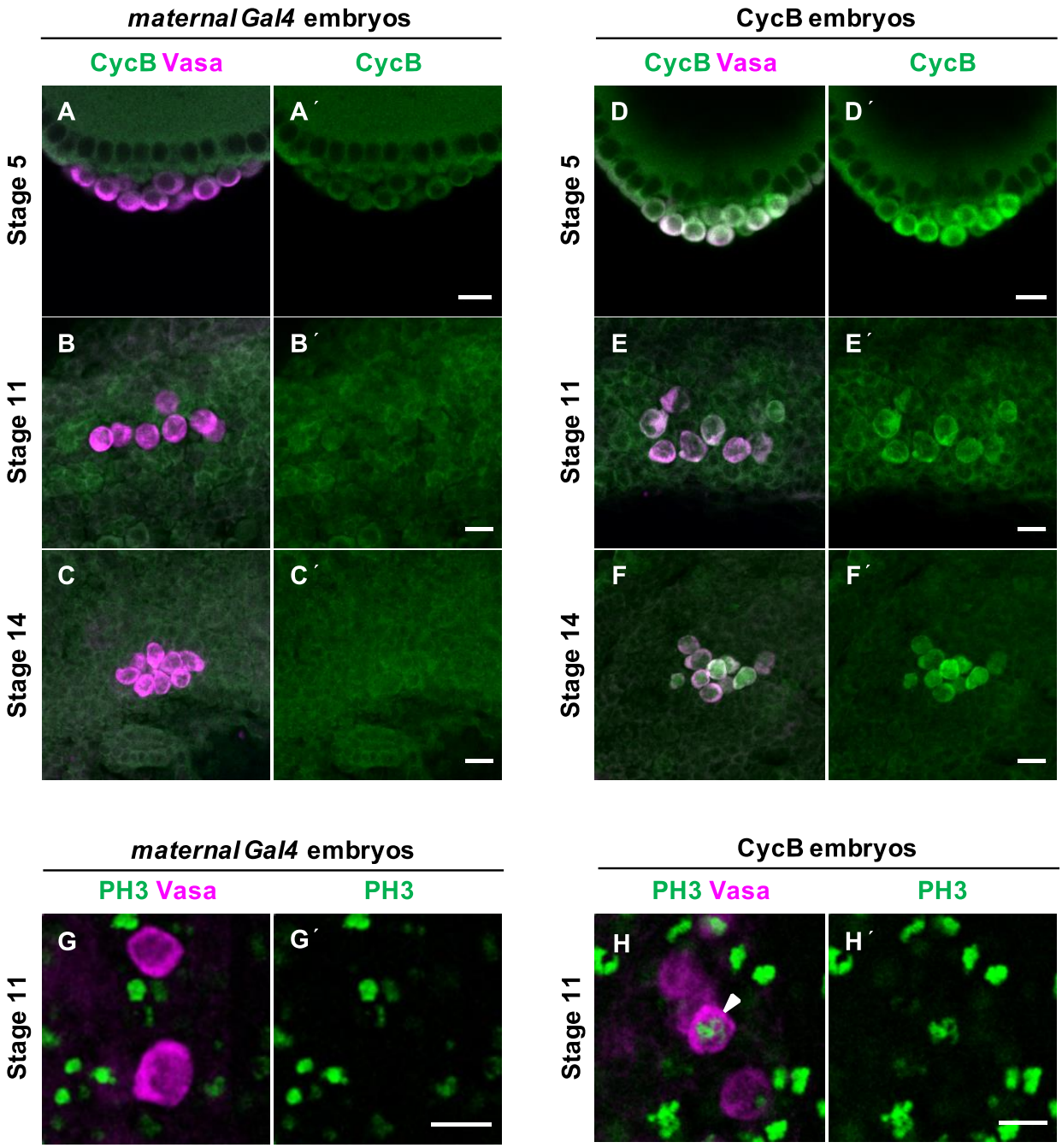

(A–F and A´–F´) Stage 5 (A, A´, D, and D´), stage 11 (B, B´, E, and E´), and stage 14 (C, C´, F, and F´) embryos derived from females with one copy of *maternal-Gal4* (*maternal-Gal4*; A–C and A´–C´) and females with one copy each of *maternal-Gal4* and *UASp-CycB-nos3´UTR* (CycB

embryos; D–F and D´–F´) were immunostained for CycB (green) and Vasa (magenta). Scale bars: 10 µm. **(G, G´, H, and H´)** *maternal-Gal4* (G and G´) and CycB (H and H´) embryos at stage 11 were immunostained for PH3 (green) and Vasa (magenta). White arrowhead indicates a PH3-positive pole cell. Scale bars: 10 µm.

Table S1. Primer sequences. Related to Figures 1–3

Table S2. Candidate genes targeted by miR-10404. Related to Figure 2 and 3

Table S3. Transcripts differentially expressed in pgc- pole cells, compared to EGFP-vas pole cells. Related to Figure 2

References

Asaoka-Taguchi, M., Yamada, M., Nakamura, A., Hanyu, K., and Kobayashi, S. (1999). Maternal Pumilio acts together with Nanos in germline development in *Drosophila* embryos. Nat. Cell Biol. *1*, 431–437.

Bischof, J., Maeda, R.K., Hediger, M., Karch, F., and Basler, K. (2007). An optimized transgenesis system for *Drosophila* using germ-line-specific *Φ*C31 integrases. Proc. Natl. Acad. Sci. *104*, 3312–3317.

Bray, N.L., Pimentel, H., Melsted, P., and Pachter, L. (2016). Near-optimal probabilistic RNA-seq quantification. Nat. Biotechnol. *34*, 525–527.

Brown, N.H., and Kafatos, F.C. (1988). Functional cDNA libraries from *Drosophila* embryos. J. Mol. Biol. *203*, 425–437.

Chak, L., Mohammed, J., Lai, E.C., Tucker-Kellogg, G., and Okamura, K. (2015). A deeply conserved, noncanonical miRNA hosted by ribosomal DNA. RNA *21*, 375–384.

Hayashi, M., Shinozuka, Y., Shigenobu, S., Sato, M., Sugimoto, M., Ito, S., Abe, K., and Kobayashi, S. (2017). Conserved role of Ovo in germline development in mouse and *Drosophila*. Sci. Rep. *7*, 40056.

Kim, D., Chang, H.R., and Baek, D. (2017). Rules for functional microRNA targeting. BMB Rep. *50*, 554–559.

Koch, R., Ledermann, R., Urwyler, O., Heller, M., and Suter, B. (2009). Systematic Functional Analysis of Bicaudal-D Serine Phosphorylation and Intragenic Suppression of a Female Sterile Allele of *BicD*. PLoS One *4*, e4552.

Robinson, M.D., McCarthy, D.J., and Smyth, G.K. (2009). edgeR: a Bioconductor package for differential expression analysis of digital gene expression data. Bioinformatics *26*, 139–140.

Sano, H., Nakamura, A., and Kobayashi, S. (2002). Identification of a transcriptional regulatory region for germline-specific expression of *vasa* gene in *Drosophila melanogaster*. Mech. Dev. *112*, 129–139.

Schindelin, J., Arganda-Carreras, I., Frise, E., Kaynig, V., Longair, M., Pietzsch, T., Preibisch, S., Rueden, C., Saalfeld, S., Schmid, B., et al. (2012). Fiji: an open-source platform for biological-image analysis. Nat. Methods *9*, 676–682.

Shigenobu, S., Arita, K., Kitadate, Y., Noda, C., and Kobayashi, S. (2006). Isolation of germline cells from *Drosophila* embryos by flow cytometry. Dev. Growth Differ. *48*, 49–57.